



UNIVERSIDAD NACIONAL AUTÓNOMA DE MÉXICO

INSTITUTO DE ENERGÍAS RENOVABLES

INSTITUTO DE INGENIERÍA

ESCUELA NACIONAL DE ESTUDIOS SUPERIORES-JURIQUILLA

Evaporative Cooling in the Instituto de Energías Renovables

THESIS

That to obtain the degree of
Ingeniera en Energías Renovables

P R E S E N T S

Jessica Nevárez Barrera

THESIS TUTOR / THESIS CO-TUTORA

Dr. Guillermo Barrios del Valle & Dra. Miriam Verónica Cruz Salas

Temixco, Mor., Junio 6 2025



Acronyms

ACL	Access Control List
CFD	Computational Fluid Dynamics
DEC	Direct Evaporative Cooling
HFMEC	Hollow Fiber Membrane-based Evaporative Cooler
HVAC	Heating, Ventilation, and Air Conditioning
IEC	Indirect Evaporative Cooling
IER	Instituto de Energías Renovables
PDEC	Passive Down-draft Evaporative Cooling
GEE-IER	Energy in Buildings group at IER

Nomenclature

δt	Time interval
δt	Time interval
\dot{m}	Mass flow
\dot{m}	Mass flow
\dot{Q}_i	Internal loads
\dot{Q}_i	Internal loads
$\rho_{\text{air},z}$	Air density in zone
$\rho_{\text{air},z}$	Air density in zone
ρ_{air}	Zone air density
ρ_{air}	Zone air density
A	Surface area
A	Surface area
C_p	Zone air specific heat capacity
C_p	Zone air specific heat capacity
C_T	Sensible heat capacity
C_T	Sensible heat capacity
C_w	Specific heat capacity of air
C_w	Specific heat capacity of air
C_z	Zone air heat capacity
C_z	Zone air heat capacity
C_p	Heat capacity under constant water vapor pressure
C_p	Heat capacity under constant water vapor pressure
h	Enthalpy
h	Enthalpy
h_g	Air enthalpy
h_g	Air enthalpy
h_s	Water vapor enthalpy
h_s	Water vapor enthalpy
$m.d.$	Maximum difference
$m.d.$	Maximum difference
m_a	Mass of dry air
m_a	Mass of dry air
m_g	Maximum amount of water vapor that air can hold at the same temperature as the mass of water

m_g	Maximum amount of water vapor that air can hold at the same temperature as the mass of water
m_s	Mass of water vapor
m_s	Mass of water vapor
m_{splus}	Mass of evaporated water added in a evaporative cooling process
m_{splus}	Mass of evaporated water added in a evaporative cooling process
n	Amount of gas substance
n	Amount of gas substance
P	Pressure
P	Pressure
P_a	Dry air pressure
P_a	Dry air pressure
P_g	Saturated water vapor pressure
P_g	Saturated water vapor pressure
P_s	Water vapor pressure
P_s	Water vapor pressure
R	Ideal gas constant
R	Ideal gas constant
R_s	Water vapor gas constant
R_s	Water vapor gas constant
R_{da}	Dry air gas constant
R_{da}	Dry air gas constant
RH	Relative Humidity
RH	Relative Humidity
$std.$	standard desviation
$std.$	standard desviation
T	Temperature
T	Temperature
t	time
t	time
T_s	Zone surface temperature
T_s	Zone surface temperature
T_z	Thermal zone temperature
T_z	Thermal zone temperature
T_∞	Outside air temperature
T_∞	Outside air temperature
T_{sup}	Supply temperature from a air system output
T_{sup}	Supply temperature from a air system output
T_{as}	Adiabatic saturation temperature
T_{as}	Adiabatic saturation temperature
T_{db}	Dry bulb temperature
T_{db}	Dry bulb temperature
T_{wb}	Wet bulb temperature
T_{wb}	Wet bulb temperature
V	Volumen
V	Volumen

V_z	Zone Volume
V_z	Zone Volume
w	Specific humidity
w	Specific humidity
w_d	Wind direction
w_d	Wind direction
w_s	Wind speed
w_s	Wind speed
W_∞	Moisture content of outside air
W_∞	Moisture content of outside air
MAE	Mean Absolute Error
MAE	Mean Absolute Error

Contents

List of Figures	ii
List of Tables	iii
1 Introduction and objectives	1
1.1 Objectives	2
2 Literature review	3
3 Methodology	8
3.1 Evaporative cooling process	8
3.2 Adiabatic mix	15
3.3 Evaporative and adiabatic process	19
4 Results	21
4.1 Evaporative cooling process	21
4.2 Adiabatic process	23
4.3 Evaporative and adiabatic process	27
5 Conclusion and Outlook	30

List of Figures

3.1	Variables on psychrometric chart with T_{db} in vertical red line, w in horizontal black line, T_{wb} in diagonal orange line, h in diagonal blue line, T_{as} as the red point and RH in dashed black line.	11
3.2	Add_water function flowchart	13
3.3	Final_Temp function flowchart	14
3.4	Building Model Created in SketchUp Representing the IER Cafeteria Structure with a Volume of 450.5 m ³ , featuring two main windows oriented toward the East and West. Left: Building model facing the exterior window of the building, known as the cafeteria lattice of the IER. This is the window through which the wind enters. Right: Building model facing the interior window of the building, where the wind exits. In both views, two additional windows are visible, each measuring 2.6 meters long by 3.5 meters high, representing the open surfaces of the cafeteria. All windows were modeled as open during the simulation.	18
4.1	Fourth experiment of Evaporative cooling process graphed on the interactive online psychrometric chart PsychroSim.	22
4.2	Experiment 1 with function adiabatic_mix and EnergyPlus simulation. Left: Inside dry bulb temperature results. Right: Inside relative humidity results.	25
4.3	Experiment 2 with function adiabatic_mix and EnergyPlus simulation. Left: Inside dry bulb temperature results. Right: Inside relative humidity results.	26
4.4	Experiment 3 with function adiabatic_mix and EnergyPlus simulation. Left: Inside dry bulb temperature results. Right: Inside relative humidity results.	26
4.5	Experiment 4 with function adiabatic_mix and EnergyPlus simulation. Left: Inside dry bulb temperature results. Right: Inside relative humidity results.	26
4.6	Experiment 5 with function adiabatic_mix and EnergyPlus simulation. Left: Inside dry bulb temperature results. Right: Inside relative humidity results.	26
4.7	Experiment 6 with function adiabatic_mix and EnergyPlus simulation. Left: Inside dry bulb temperature results. Right: Inside relative humidity results.	27
4.8	Experiment 7 dry bulb temperature and relative humidity results. Left: Inside dry bulb temperature results. Right: Inside relative humidity results.	27
4.9	Adiabatic mix and evaporative cooling experiments - One minute of evaporation. Blue line are outdoor conditions. Dotted yellow line are indoor conditions computed by .py file in EnergyPlus. Dotted green line are indoor conditions computed by Python function. a) Inside dry bulb temperature behavior. b) Inside relative humidity variable behavior. d) Inlet air mass variable behavior.	28
4.10	Adiabatic mix and evaporative cooling experiments - Five minutes of evaporation. Blue line are outdoor conditions. Dotted yellow line are indoor conditions computed by .py file in EnergyPlus. Dotted green line are indoor conditions computed by Python function. a) Inside dry bulb temperature behavior. b) Insie relative humidity variable behav-ior. d) Inlet air mass variable behavior.	29

List of Tables

3.1	Evaporative process experiments. Initial conditions of dry bulb temperature and relative humidity (T_{dbi} , RH_i) and the amount of kilograms of evaporated water added into the air ΔH_{2o}	14
4.1	Results of evaporative cooling process experiment	22
4.2	Adiabatic process experiments	24
4.3	Mean Absolute Error (MAE), standard desviation (std.) and maximum difference (m.d.) of adiabatic process experiments results.	25
4.4	Mean Absolute Errors (MAE), standard deviation (std.), and maximum difference (m.d.) for the comparison experiment results of the variables T_{db} and RH	29

Chapter 1

Introduction and objectives

It is often said that the cleanest energy is the one that is not used. A clear example of this is bioclimatic architecture. It employs techniques, some of which are quite ancient, to make the most of available resources, climatic conditions, and available space. These methods include strategies for improving indoor temperature and humidity, both of which are essential for ensuring thermal comfort. Due to the high energy demand of Heating, Ventilation, and Air Conditioning (HVAC) systems, low-energy-consumption air-cooling techniques are a valuable resource to reduce electricity consumption. One of these techniques is evaporative cooling. This technique utilizes heat transfer from air to water for its evaporation, resulting in a decrease in the air temperature. Although it may seem like a fairly common method, its study has been limited due to the lack of a simulation process capable of modeling evaporative cooling inside buildings over extended periods (e.g. a year) while simultaneously incorporating additional considerations and other bioclimatic design techniques.

Simulations are an excellent and widely used technique for experimentation and optimization. They allow for the exploration of bioclimatic design techniques in specific cases to determine which would be more feasible. Whole building simulations are frequently used in Instituto de Energías Renovables (IER). One of the software programs aimed at this type of study in buildings is EnergyPlus (Laboratory, 2025). EnergyPlus is an open source software that simulates thermal performance of a building considering construction materials, orientation, airflow, etc. The current problem, which this thesis works on, is that EnergyPlus does not have modules to calculate direct evaporative cooling using water sprayers.

The objective of this thesis is to develop a methodology with an algorithm for direct evaporative cooling in an adiabatic space by sprayers and validate it. Once validated, this algorithm will be used to compare it with another simulation process in EnergyPlus developed by the Energy in Buildings group at IER (GEE-IER). GEE-IER is working on building a model that addresses the conditions caused by direct evaporative cooling using water sprayers. Once a validated model is obtained, the group's next step will be to compare the results with temperature and humidity measurements taken from a space equipped with a physical sprayer-based evaporative cooling system.

1.1 Objectives

General objective:

Develop a methodology to validate the direct evaporative cooling algorithms implemented in Energy-Plus.

Specific objectives:

- Review of the literature on evaporative cooling in buildings and EnergyPlus.
- Understand and calculate the psychrometric measurements for the evaporative cooling process.
- Develop and validate a methodology and an algorithm that incorporates evaporation of water and adiabatic air mixing in a space.
- Use the validated algorithm to review possible evaporative cooling algorithms implemented in EnergyPlus.

Chapter 2

Literature review

The physical phenomena of evaporative cooling consist in water evaporation into the air; the latent energy needed by the water to evaporate is transferred from the air. This causes a decrease in dry bulb temperature and an increase in moisture in the surrounding air (Çengel, 2012). Evaporative cooling is an adiabatic process because it does not require any heat or work supply and the heat transfer between air and water is negligible.

In order to take advantage of this effect, several implemented systems that use evaporative cooling to achieve specific temperature and humidity depending on the sector, the kind of technology and the objective.

Widely used in building applications to reduce temperatures especially in warm and dry environments, evaporative cooling is considered as one of the cheapest and oldest cooling technologies (Santamouris & Kolokotsa, 2013) and it requires a quarter of the electric power of a mechanical vapor-compression system according to Mohammad et al. (2013). This last idea is of high relevance due to the levels of greenhouse gases (GHGs) that Heating, Ventilation, and Air Conditioning (HVAC) systems produce and the amount of efforts focused on the search and development of friendlier environmental technology to maintain human thermal comfort in buildings. Over the past three decades, from 1990 to 2022, indirect carbon dioxide (CO_2) emissions resulting from space cooling in buildings have nearly tripled worldwide, reaching almost 1 Gton, as reported by the International Energy Agency (IEA, 2023), and its reduction is not predicted yet. These increments could be caused by many factors such as urbanization, more accessibility to HVAC systems and the temperatures increment due climate change.

An example of the importance of evaporative cooling systems is the urban heat island effect. It is a phenomenon produced in cities where abound infrastructure such as buildings and roads that absorb and re-emit the sun's heat more than natural landscapes causing higher temperatures within this "island" than outlying areas. In the presence of this phenomenon, human health can be compromised in the absence of an efficient, accessible, and low energy cost building cooling system (Meng et al., 2022).

Summarizing, evaporative cooling systems have become more demanded and in some cases crucial to mantain thermal comfort in open spaces where a conventional HVAC system would not be efficient. It is needed that these systems become more efficient and use technology with less consumption of resources and less CO_2 emissions like evaporative cooling systems.

Evaporative cooling systems are commonly divided in two categories; Indirect Evaporative Cooling (IEC) and Direct Evaporative Cooling (DEC). The purpose of IEC is to decrease temperature without increasing moisture. This aims to cool the occupied room through evaporative cooling while keeping the moist air separated from it using heat exchangers. An example of this technology is the one described by Santamouris and Kololotsa in their state of art of passive cooling dissipation techniques for buildings and other structures (Santamouris & Kolokotsa, 2013). According to them, configurations of IEC systems can reach an effectiveness of almost 75%.

There are more complex mechanisms such as cross-flow indirect evaporative air cooler explained by Duan et al. (2019). This system consists of several plates, with one side dry and the other wet; evaporative cooling occurs on the wet side, while the heat required for this process is transferred through the dry side. As a result, the air on the dry side becomes cooler without an increase in moisture.

Compared to other passive technologies, IEC is also very convenient. Krüger et al. (2010) analyzed indoor temperature monitoring of a building with high thermal mass and the indoor temperature predictions of a second building that uses IEC. They showed that, although both methods are beneficial from a thermal point of view, the IEC case resulted in no cooling requirement, unlike the high thermal mass method. On the other hand, compared with active technologies, it also has shown promising results. Jaber & Ajib (2011) estimated savings of about 1,084 GWh/year and 637,873 Ton of CO_2 annually avoided once using an IEC in 50,000 Mediterranean residential buildings instead of traditional HVAC systems. In both articles IEC systems present excellent results, although the regions where the experiments are implemented have a warm and humid climate, or humid by seasons.

The other category of evaporative cooling is DEC. There are several methods of DEC and the mechanism is pretty simple. It consists of air passing through a humid medium. Water of the humid area evaporates due latent heat transfer between the air and the water. The result is an air temperature decrease and humidity increase because of the water vapor added. Within these systems there are pads, Passive Down-draft Evaporative Cooling (PDEC) towers and water spray cooling systems.

Pads are one of the most common DEC methods in which factors such as the kind of material or air gaps between pads are analyzed. Al-Sulaiman (2002) conducted several experiments to evaluate the natural fibers used in pads, showing a highest efficiency of 62.1% for jute, an affordable natural fiber. On the other hand, Zhang et al. (2022) made a Fluent simulation to model the heat and mass transfer process in a medium-gap-medium arrangement of wet a medium, demonstrating, among other conclusions, that air speed is fundamental in the evaporative cooling process.

Another well studied DEC systems are PDEC towers. These systems are typically attached aside of a building and contains water sprayers. The air enters the tower and it is cooled by DEC. Kang & Strand (2019), through simulations, determined that PDEC towers are capable of conditioning building spaces in dry climates and warm moderate climates. Even under the conditions established in the article, this technology could be the primary cooling system. However, inlet mass flow rate is a key factor for the performance of these kinds of systems.

DEC systems in which this thesis work is focused on are water spray cooling systems. Consist of sprayers located commonly at the ceiling of a ventilated room that are widely used due to their efficient cooling performance and easy control. Several experiments have shown sprayers could increase thermal comfort. Meng et al. (2022) showed statistical results where water spray cooling systems have a representative cooling range was from 1 to 9 °C.

The main difference between DEC and IEC is the final air moisture content. While the DEC increases the relative humidity, the IEC keeps the moisture separate from the space (Mohammad et al., 2013). Deciding which of the two to implement can depend on their cost, availability, but above all, climate must be taken into account. According to Santamouris & Kolokotsa (2013), IEC can achieve an effectiveness of almost 75% and is great to implement in hot and humid climates because they do not increase moisture content. In these conditions, DEC is not as effective as IEC; this technology should be used in hot and dry climates, where it can achieve an effectiveness of 50–70%. Nevertheless, DEC is cheaper and easier to implement.

DEC is a technology widely studied. There have been both experimental and numerical experiments elaborated with the aim of studying its performance and the key factors that affect it. In experimental investigations documented in the literature, Alaidroos & Krarti (2016) developed a water spray cooling system in a controlled laboratory setting. Various tests were conducted by altering the climate conditions within the room. The most significant outcome was the reduction of air temperature from 45 to 25.5°C. Another important set of experimental results was generated by Huang et al. (2011) through an analysis of monitoring data from water spray cooling systems installed in locations with varying climate conditions. According to these results, a spray cooling system can reduce air temperature between 5 and 7°C when the ambient temperature is 35°C and the relative humidity is approximately 45%.

While experimental studies can provide insights into the performance of a spray cooling system in a desired installation location, simulations are essential to evaluate the system under various conditions and making more informed decisions. As the main objective of this thesis work is to propose a methodology to validate algorithms to be implemented in whole building simulations, it is important to explore the existing literature in this area. This mean, examining the types of spray cooling system simulations already available and determining if they are suitable for the requirements of new investigations.

Most of DEC simulations found in literature are made with Computational Fluid Dynamics (CFD), the following authors reported CFD: Zhang et al. (2022) utilized CFD to study the effect of different pads arrangement on temperature and humidity parameters. Alkhedhair et al. (2013) and Kang & Strand (2013) utilized it to estimate the key parameters that affect the cooling performance of PDEC towers. Also, Kang & Strand (2013) used CFD to model the heat and mass transfer of the phenomenon as a turbulent flow and concluded that DEC systems have a high climatic dependency; the more humidity is in the air, the performance gets more compromised.

On the other hand, CFD has also been used to study the effect of droplet size on evaporation performance (Alkhedhair et al., 2013) or other parameters such as spray angle and water mass flow rate (Raoult et al., 2019). There are articles that make CFD simulations to analyze the performance of more complex systems, like the one made by Jafari & Kalantar (2022) which simulates a combination of a wind catcher, solar chimney and spray cooling systems.

These studies bring rich conclusions about DEC systems performance, however CFD systems are not able to analyze whole buildings with these systems integrated due the amount of computational work. Besides, these kinds of simulations deliver good results in a brief period of time and with less complex equipment compared to a whole building.

To see spray cooling systems interaction with a building, the energy transfer with more thermal zones, electric equipment and other thermal loads in a large period of time like a year, it is necessary to appeal to other types of simulations.

Yan et al. (2022) developed prediction models for an hollow fiber membrane-based evaporative cooler Hollow Fiber Membrane-based Evaporative Cooler (HFMEC) performance with statistical method. Although results look promising using regression models, the interaction between DEC systems with the building still is not considerate. Besides, the article studies a DEC system based on pads with a single airflow direction. Alternatively, Anbarasu et al. (2022) used Modelica program to develop a physics-based model to compute heat and mass transfer of DEC systems with pads too. Although their experiment also aims to simulate DEC pad systems, it utilises EnergyPlus to make the validation.

EnergyPlus is an open source software developed by the Department of Energy of the US Government since 1997 (Luigi Gentile Polese, 2014). By a collection of program modules it computes a whole building energy simulation in large periods of time and brief time steps (up to a minute). It is able to make simulations under different environmental, constructional and operating conditions. It is widely used to investigate the effects of air cooling technologies in different conditions. It could be an excellent tool for analyzing the impact of spray cooling systems on thermal comfort within buildings.

Regarding evaporative cooling systems, EnergyPlus has six objects to simulate evaporative cooling systems (both indirect and direct); however, none of them can simulate an evaporative cooling system by the dispersion of water particles inside the room intended for cooling. EnergyPlus has an Indirect Evaporative Cooler and some input objects. The Indirect Evaporative Cooler supplies two air flows to avoid humidity increase in the room, as in the Duan et al. (2019) indirect cooler. On the other hand, there are also input objects; IEC wet coils and IEC dry coils. Both methods utilises exchangers too. The difference between these two is how the secondary airflow is cooled: while the dry coil uses humid pads, the wet coil uses sprayers.

In addition, EnergyPlus includes objects to simulate DEC systems. Includes objects such as Direct Evaporation Cooler, cooling towers, and ZoneHVAC:EvaporativeCoolerUnit. The Direct Evaporation Cooler is operated with pads. It cannot be used to simulate spray cooling systems with due it is an unidirectional airflow operation, and the evaporation ratio can vary from pads to drops. This object is used by Naderi et al. (2020) and Chiesa et al. (2017) to compare the effectiveness of these systems in different geographical areas with different climate conditions, resulting in an efficient technology especially in hot and dry places.

Cooling towers, classified as DEC, can be simulated using EnergyPlus too. Chiesa used it to compare the results with experimental data and Kang & Strand (2018, 2019), used this object to study its performance in different climates and operations.

Finally, EnergyPlus also has the object ZoneHVAC:EvaporativeCoolerUnit that couples a fan and one or two evaporative coolers in a zone unit. Tewari, S. Mathur & J. Mathur (2019) used it to predict the thermal performance of an office building in India during summer, revealing that it could reduce discomfort between 42 and 52%. Although these three objects are DEC (Direct Evaporation Cooler, cooling towers, and ZoneHVAC:EvaporativeCoolerUnit), they cannot be used to simulate spray cooling systems for a simple reason. Their mechanisms operate based on a single airflow direction, unlike spray cooling systems, which are typically installed in open areas with airflow coming from multiple directions.

In spray cooling systems, airflow could have different directions because they do not have a mechanical system designed so that air passes specifically through it and are usually installed in open spaces. In the case of pads, cooling tower, and the evaporative unit, they are designed to have a single airflow direction in order to pass over the system first and then enter to the room. For this reason, it is needed to

create a simulation model for water spray cooling systems in EnergyPlus and a methodology to validate the model due to the complex heat and mass transfer occurring in a building; to make it work along AirFlowNetwork. AirFlowNetwork model in EnergyPlus simulates natural ventilation. These would be better suited to the real physics occurring in DEC spray systems and provide more reliable results. The issue here is that EnergyPlus does not have a module to simulate DEC water spray cooling systems.

Water spray cooling systems simulations are still a challenge in development. Simulations have become a transcendent tool in the study of energy in buildings. It is easier to estimate the effect that systems would have on thermal comfort within a building without making a real installation and to make more informed decisions of what technology to use considering the economic and environmental cost. This is the reason why it is essential to create a reliable simulation tool for water spray cooling systems to give them visibility, and to bring them to the attention of the public as a more sustainable cooling technology for an increasingly cooling technology-dependent world.

Chapter 3

Methodology

This chapter presents the methodology for creating an algorithm that simulates direct evaporative cooling through water spray cooling systems and mixing of air simultaneously in an adiabatic space. This algorithm will be used to validate the methodology developed by the IEC's building group.

To achieve this, two functions were coded in Python: The first function calculates the DEC of the air, while the second determines the temperature and humidity conditions resulting from the adiabatic mixing of two volumes of air. Once both functions were created, the next step is to combine them in order to have a single and robust function coded in Python that computes DEC by a water spray cooling system in an adiabatic open space. First and second functions are described in section 3.1 and 3.2.

3.1 Evaporative cooling process

This section aims to describe the process of creating the first function that calculates the resulting dry bulb temperature and relative humidity when spraying water in an air volume. This process involves the psychrometric equations, the flowchart of the algorithm used to create the function, the Python code development of the function and the assumptions devised to achieve a closer approximation to reality.

3.1.1 Psychrometry concepts

Here are presented the fundamental psychrometric terms and the equations that were taken into account to create the algorithms for simulating evaporative cooling by spray cooling systems. Each of the following equations and definitions is taken from Cengel (2012).

Psychrometrics is the study of the thermodynamic properties of atmospheric air, which is characterized by containing a certain amount of water vapor. The air that does not contain water vapor is referred as dry air. An advantage of air conditioning applications is that they typically operate at temperatures below 50°C, allowing both air and water vapor to be treated as ideal gasses (with the error in the case of water vapor being less than 0.2 percent). Therefore, both gasses obey the ideal gas law,

$$PV = nRT, \quad (3.1)$$

where:

- P : Pressure [Pa].
- V : Volumen [m^3].
- n : Amount of gas substance [mol].
- R : Ideal gas constant, 8.314 [J/mol*K].
- T : Temperature [K].

As ideal gases, air and water vapor obey Dalton's law of partial pressures, which states that the sum of the partial pressures of the gases equals the total pressure of the mixture,

$$P = P_a + P_s, \quad (3.2)$$

where:

- P_a : Dry air pressure [Pa].
- P_s : Water vapor pressure [Pa].

The equations 3.1 and 3.2 will allow us to determine the mass of water present in the air, given its temperature, pressure, and volumen. Similarly, as an ideal gas, it is possible to determine the water vapor enthalpy (h_s) because it just depends on the temperature under constant pressure conditions. This will be almost equal to the enthalpy of saturated air at the same temperature,

$$\begin{aligned} h_s(T) &\cong h_g(T), \\ h_g(T) &\cong h_g(0^\circ C) + Cp * T, \end{aligned} \quad (3.3)$$

where:

- $h_g(0^\circ C)$: Saturated air enthalpy at $0^\circ C$, 2500.9 [kJ/kg].
- Cp : Heat capacity of water vapour under constant pressure, 1.82 [kJ/C*kg].
- T : Gas temperature [$^\circ C$].

To describe the amount of water vapor in the air, there are two variables that describe it: specific humidity (w) and relative humidity (RH). Specific humidity represents the ratio of the mass of water in a unit of dry air (eq. 3.4). This value can be expressed in terms of the ideal gas law,

$$w = \frac{m_s}{m_a}, \quad (3.4)$$

$$w = \frac{P_s/R_s}{P_a/R_a} = 0.622 \frac{P_s}{P_a}, \quad (3.5)$$

where:

- m_s : Mass of water vapor [kg].
- m_a : Mass of dry air [kg].
- R_s : Water vapor gas constant, 461 [J/mol*K].
- R_a : Dry air gas constant, 287 [J/mol*K].

On the other hand, relative humidity is the ratio of the mass of water present in the air to the maximum amount of water that the air can hold at the same temperature (eq. 3.6). When the relative humidity (RH) is 100%, the air is saturated and cannot hold any more water,

$$RH = \frac{m_s}{m_g} = \frac{P_s}{P_g}, \quad (3.6)$$

where:

- m_g : Maximum amount of water vapor that air can hold at the same temperature as the mass of water [kg].
- P_g : Saturated water vapor pressure [Pa].

Other crucial variables for the evaporative cooling calculations are temperatures. The temperature measured by a thermometer in the open air is called the dry bulb temperature (T_{db}), also known as the ordinary atmospheric air temperature. On the other hand, if the thermometer is covered with a piece of wet cotton and air blows over it, the temperature indicated by the thermometer is called the wet bulb temperature (T_{wb}). This temperature is approximately equal to the adiabatic saturation temperature (T_{as}); however, they have different concepts. The T_{as} is determined from an adiabatic humidification process, meaning that the moisture content of the air increases without the intervention of any external work or heat source. This moisture content comes from the evaporation of water present in the volume of air, which takes heat from the air itself to evaporate. As the air transfers heat to the water for its evaporation, its temperature decreases and its relative humidity increases. When the relative humidity reaches 100% due to the amount of evaporated water, the air reaches T_{as} .

These variables described above and how they relate each other can be identified on the psychrometric chart. The psychrometric chart is a graphical and easy-to-read representation of the psychrometric formulas presented earlier. In figure 3.1 there is presented a psychrometric chart, and the variables are explained as follows:

- T_{db} : vertical red line.
- w : horizontal gray line.
- h : diagonal blue line.
- RH : dotted line.
- T_{wb} : diagonal orange line.
- T_{as} : red point.

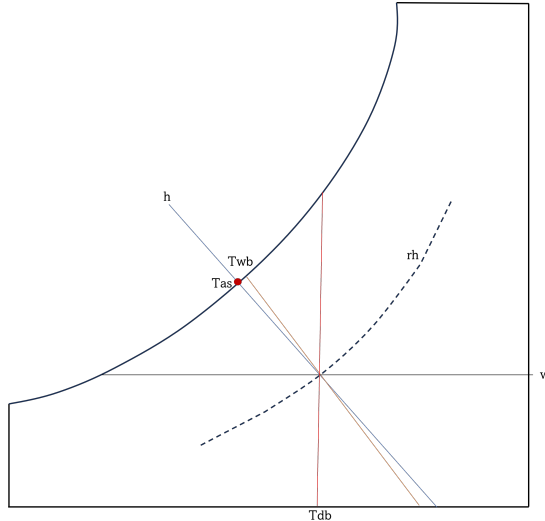


Figure 3.1: Variables on psychrometric chart with T_{db} in vertical red line, w in horizontal black line, T_{wb} in diagonal orange line, h in diagonal blue line, T_{as} as the red point and RH in dashed black line.

The blue line represents evaporative cooling; an increase in RH and a decrease in T_{db} while the enthalpy remains constant.

To calculate the final T_{db} and the final RH of an evaporative cooling process from these same initial variables, the following variables must be determined: vapor pressure of water (P_v), the mass of water vapor (m_s) and the mass of dry air (m_{da}), and the enthalpy of the atmospheric air (h). P_v is obtained from equations 3.2 and 3.6. To determine m_s and m_a , equation 3.1 was utilized, using mass instead of moles and the respective gas constants,

$$m_{da} = \frac{P_a V}{R_{da} * T_{db}}, \quad (3.7)$$

$$m_s = \frac{P_s V}{R_s T_{db}}, \quad (3.8)$$

where:

- R_{da} : 287.042 [J/kgK].
- R_s : 461 [J/kgK].
- V : Volumen [m^3].

Once obtained the mass of dry air and water vapor, it is possible to determine the specific humidity of the air with the mass of evaporated water added (w_2),

$$w_2 = \frac{m_s + m_{splus}}{m_{da}}, \quad (3.9)$$

where:

- m_{splus} : Mass of evaporated water added.

Then, w_2 is used then to calculate the dry bulb temperature at the end of the evaporative cooling process (T_{db2}):

$$T_{db2} = \frac{h/1000 - 2500.9 * w_2}{1.006 + 1.86 * w_2}. \quad (3.10)$$

The enthalpy can be calculated with equation 3.3. The next step is to calculate the water vapor pressure at the end of the evaporative cooling process (P_{v2} using equations 3.2 and 3.5 as follows:

$$P_{v2} = \frac{Pw_2}{0.622 + w_2}. \quad (3.11)$$

Having P_{v2} will allow us to determine the final relative humidity (RH_2) with equation 3.6. This is the calculation process utilized to create a function that obtains the T_{db} and the RH of the air after an evaporative cooling process.

3.1.2 Code development

This section describes the developing process and the assumptions taken into account to create an algorithm that computes the resulted T_{db} and resulted RH from a DEC by sprayers. The value of the psychrometric variables are calculated using the library psychrolib.py (Meyer & Thevenard, 2019). This open-source library contains functions from the ASHRAE Handbook fundamentals (American Society of Heating & Engineers, 2017) for calculating thermodynamic properties of gas-vapor mixtures. It is available for different programming languages including Python among its user guide on GitHub (2024).

The function developed to compute the direct evaporative cooling process was created using the following approach: In an adiabatic room, a specific amount of water is introduced and completely evaporated. The resulting water vapor mixes with the air, raising the relative humidity and lowering the dry bulb temperature of the air in an isenthalpic process. The assumptions made to create this function were:

- The air and water vapor are considered as ideal gases.
- The entire quantity of water added to the air is completely evaporated.
- It is a closed volume, and there is no infiltration of air; therefore, the air mass remains constant.
- It is an isenthalpic process.
- The volume of the room is $1m^3$, therefore, the volumen of air is also $1m^3$.

The flowchart in Figure 3.2 illustrates the process flow of the first function, named Add_water. This function requires the initial air conditions and the amount of water to be added. The initial conditions are dry bulb temperature, relative humidity, and air pressure, which are essential for determining the air's initial state (at least three psychrometric variables are needed to determine the remaining ones as the enthalpy). This is an adiabatic isenthalpic process, meaning that, since there is no heat or work input, the enthalpy remains constant. To compute the final dry bulb temperature and relative humidity,

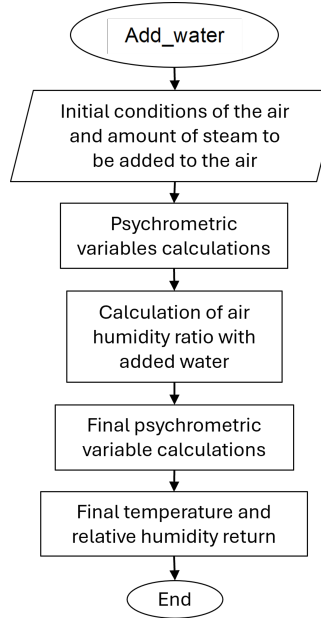


Figure 3.2: Add_water function flowchart

it is necessary to perform a mass balance by incorporating the amount of water added to the air. The amount of water corresponds to the quantity released by the sprayers, assuming complete evaporation and incorporation into the air. Upon performing these calculations, the Add_water function returns the final dry bulb temperature and the final relative humidity resulting from the evaporative cooling process.

The function Add_water computes a simple process, however, if the air reaches its saturation point (where relative humidity equals 100% and it cannot hold more water), the results given are not physically accurate because the function continues adding water into the air. To calculate the physically correct variables another function, Final_Temp, was developed. This last function handles the following different scenarios:

- No water was added, so there is no evaporative cooling.
- Water is added and air does not reach the saturation point.
- Water was added, air reaches the saturation point and the remaining water cannot evaporate.

The Figure 3.3 illustrates the flowchart of the Final_Temp function. In order to address the previously mentioned scenarios, Final_Temp computes the adiabatic saturation temperature, which represents the temperature at the saturation point following an isoenthalpic process such as DEC. This variable allows for the computation of other psychrometric variables at the saturation point. Subsequently, the function determines the required amount of water to achieve saturated air and compares it with the amount of water added. After obtaining this information, the function evaluates whether the air is expected to reach the saturation point. If it is, the function calculates the amount of water remaining to evaporate. Regardless of the scenario, Final_Temp returns the final dry bulb temperature and final relative humidity, along with the amount of water evaporated and any remaining unevaporated water, if applicable.

In order to validate both functions (Add_water and Final_Temp), four tests were made with different initial conditions of dry bulb temperature and relative humidity, and the amount of water to be added,

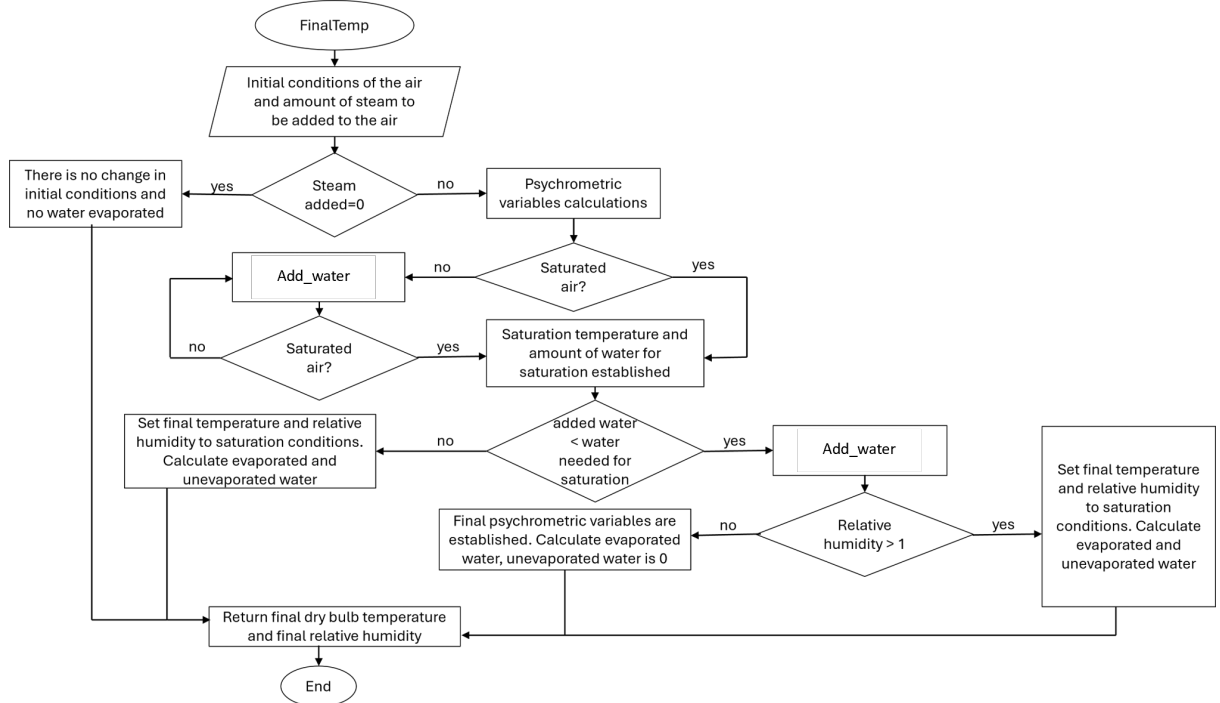


Figure 3.3: Final_Temp function flowchart

evaporated and incorporated into the air. The results will be compared with an online psychrometric chart (SimCal, 2024), made by SimCalc Development. This online chart, as the PsychroLib library used in Python, is based on ASHRAE Fundamental handbook formulas (American Society of Heating & Engineers, 2017). This will allow to know if the functions were well developed.

In table 3.1, the four experiments are presented along with their initial conditions of the inside zone air (T_{dbi} , RH_i) and the amount of evaporated water. The first two experiments aim to simulate temperatures between 20 and 30°C and relative humidity between 25 and 50% with the same amount of evaporated water. The third experiment simulates the evaporative cooling process with the same amount of water released as one row of sprinklers located in the IER's cafeteria within a minute. The last experiment aims to simulate the evaporative process with the amount of evaporated water that takes the air to saturated conditions. The validation results can be found in chapter 4.

Exp.	$T_{dbi_i}[^{\circ}\text{C}]$	$RH_i[\%]$	$\Delta H_2O[\text{kg}]$
1	20	25	0.007
2	30	50	0.007
3	30	50	0.0477
4	30	50	0.5

Table 3.1: Evaporative process experiments. Initial conditions of dry bulb temperature and relative humidity (T_{dbi} , RH_i) and the amount of kilograms of evaporated water added into the air ΔH_2o

3.2 Adiabatic mix

In this section it is presented the methodology for developing an algorithm that simulates the air conditions resulting from the combination between two volumens of air. The objective is to enhance the capabilities of the direct evaporative cooling system algorithm by incorporating air mixing. This is crucial as these systems are typically situated in open ventilated spaces where wind direction and psychrometric conditions could be continually changing. To achieve this, it was made a function, coded in Python, that performs an adiabatic mixture of two volumes of air with different conditions of dry bulb temperature and relative humidity. To create it, it was started with the energy and mass balance equations.

3.2.1 Energy and mass balance equations

In order to create an algorithm in python that performs an adiabatic mixture of two volumes of air with different conditions of dry bulb temperature and relative humidity it was firts applied energy and mass balance equations. The energy balance is represented by equation (3.12) wich is described in the Engineering Reference of EnergyPlus (Energy, 2022a) where it is explained every physical aspects that the software is based on. The change in energy in the zone air equals the sum of internal loads, convective heat transfer from the zone surfaces, heat transfer due to infiltration of outside air or interzone air mixing, and air system output (if applicable).

$$C_z \frac{dT_z}{dt} = \sum_{i=1}^N \dot{Q}_i + \sum_{i=1}^{N_{\text{surfaces}}} h_i A_i (T_{si} - T_z) + \sum_{i=1}^{N_{\text{zones}}} \dot{m}_i C_p (T_{zi} - T_z) + \dot{m}_{\text{inf}} C_p (T_{\infty} - T_z) + \dot{m}_{\text{sys}} C_p (T_{\text{sup}} - T_z), \quad (3.12)$$

where:

- $\sum_{i=1}^N \dot{Q}_i$: Sum of the convective internal loads.
- T_s : Zone surface temperature.
- T_z : Thermal zone temperature
- T_{∞} : Outside air temperature.
- T_{sup} : Supply temperature from a air system output.
- $\sum_{i=1}^{N_{\text{surfaces}}} h_i A_i (T_{si} - T_z)$: Convective heat transfer from the zone surfaces.
- $\dot{m}_{\text{inf}} C_p (T_{\infty} - T_z)$: Heat transfer due to infiltration of outside air.
- $\sum_{i=1}^{N_{\text{zones}}} \dot{m}_i C_p (T_{zi} - T_z)$: Heat transfer due to interzone air mixing.
- $\dot{m}_{\text{sys}} C_p (T_{\text{sup}} - T_z)$: Air systems output.
- $C_z \frac{dT_z}{dt}$: Energy stored in zone air.
- C_z : Zone air heat capacity.
- ρ_{air} : Zone air density.
- C_p : Zone air specific heat capacity.

- C_T : Sensible heat capacity multiplier (detailed description is provided below).

To solve the energy balance, Euler's algorithm was used due to its lower computational load and higher-order algorithms introduced an inertia effect that impacted results. This solution uses the finite difference approximation of equation (3.13),

$$\frac{dT_z}{dt} = \frac{T_z(t) - T_z(t - \delta t)}{\delta t} + O(\delta t), \quad (3.13)$$

after substituting the common arguments from both previously mentioned equations, the final step to prepare the function for implementation in Python is to simplify it. Therefore, all the removable arguments were eliminated. The sum of the convective loads and the air system output were removed in order to maintain a simple simulation for later validation; thus, they were not considered. The heat transfer due to interzone air mixing was also eliminated because it is assumed to be just one thermal zone. On the other hand, as it is an open space, heat transfer due to infiltration of outside air is not eliminated. The convective heat transfer from the zone surfaces could not be eliminated due to its complexity in EnergyPlus and will be added as a thermal load. This software serves as the validation method for this air mixing algorithm, so it was necessary to retain it. More details of this validation process will be provided in the next chapter. Finally, the resulting equation for creating a Python function is Equation 3.14,

$$T_z = \frac{\dot{m}_{\text{inf}} C_p T_{\infty} + \frac{C_z}{\delta t} T_z(t - \delta t) + \sum_{i=1}^{N_{\text{surfaces}}} h_i A_i (T_{si} - T_z)}{\frac{C_z}{\delta t} + \dot{m}_{\text{inf}} C_p}. \quad (3.14)$$

The mass balance is a similar equation, but instead of temperature, it uses the air humidity ratio. To compute the air humidity ratio resulting from a mixture of two volumes of air, the process follows the same steps as described above. It begins with an expanded air mass balance equation. Then, the Euler method was employed to solve it using finite differences, followed by a simplification. The result is shown in equation 3.15. In this case, the variable solved was the humidity ratio, which is then used in the Python function to compute the relative humidity.

$$W_{t,z} = \frac{\dot{m}_{\text{inf}} W_{\infty} + \frac{\rho_{\text{air},z} V_z C_w}{\delta t} W_z(t - \delta t)}{\frac{\rho_{\text{air},z} V_z C_w}{\delta t} + \dot{m}_{\text{inf}}}, \quad (3.15)$$

where:

- $W_{t,z}$: Humidity ratio in zone z at time t .
- $\rho_{\text{air},z}$: Air density in zone z .
- $W_z(t - \delta t)$: Moisture content in the zone the previous time step.
- \dot{m}_{inf} : Mass flow rate of infiltration air.
- W_{∞} : Moisture content of outside air.
- V_z : Volume of zone z .
- C_w : Specific heat capacity of air.

- δt : Time interval.

Summarizing, equations 3.14 and 3.15 result from solving energy and moisture balances using the Euler method and making a subsequent simplification. The next step is to develop a function in Python that can correctly compute the final dry bulb temperature and final relative humidity using these equations.

3.2.2 Code development

The previous energy and mass balance equations presented, 3.14 and 3.15, are utilized to create the Python function `adiabatic_mix`, which computes the final dry bulb temperature and relative humidity when mixing two volumes of air. For the simulation of DEC by spray cooling system, this function simulates the entry of outside air into the adiabatic zone.

To validate the correct calculation of the adiabatic mixture of two volumes of air using `adiabatic_mix`, EnergyPlus was utilized. EnergyPlus was chosen due to its comprehensive simulation capabilities for various variables, it is open-source software, and it is already widely used in the IEC. Additionally, it includes the AirFlowNetwork model, which can simulate the direction and speed of air through nodes. The validation process involved creating a simulation of an adiabatic thermal zone in EnergyPlus and ensuring that the only phenomenon occurring was air mixing between the air inside the zone and the outside air entering the zone.

3.2.3 EnergyPlus simulation

The `adiabatic_mix` function, and the rest of the functions will be used in a numerical simulation in EnergyPlus, which can handle air exchange between a space and the outdoor. So, this function will be validated in EnergyPlus because it can handle air mixing in a space. Because the function developed considers an adiabatic space, the following process was carried out. The first step in the EnergyPlus simulation was to create one thermal zone building model modeled in SketchUp. The created model is a rectangular volume of 450.5 m³, similar to the cafeteria at IER, where a DEC system has been installed. The window on the east side measures 14 x 3.5 meters, while the window on the west side measures 9.25 x 3.5 meters (see figure 3.4). Two additional windows measuring 2.6 x 3.5 m were also modeled to simulate the open area of the cafeteria. All windows were modeled to remain open during the following simulations. Before executing the numerical experiments, it was important to ensure an adiabatic environment, this means, create an adiabatic zone. To achieve this it was crucial to avoid any heat transfer in the model that was not caused by airflow. From SketchUp, an .idf file was exported and uploaded in EnergyPlus software, where the remaining actions to make it an adiabatic zone took place.

Then the following conditions were applied:

- Adiabatic condition in each zone surface.
- NoMass materials with zero thermal absorptance, zero solar absorptance, and high thermal resistance. The highest value possible was $1E^{14}$.
- Window material with U-Factor, Solar Heat Gain Coefficient and Visible Transmittance to zero.
- As the convection heat transfer on surfaces cannot be avoided, the convection coefficient was set to 0.1, the minimum value possible.

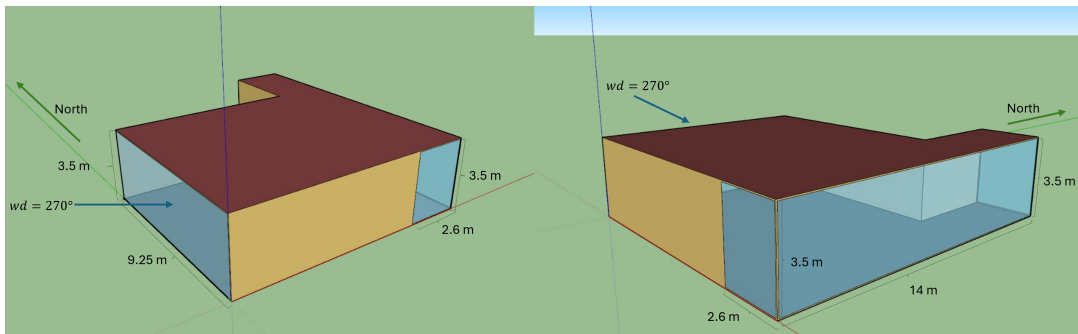


Figure 3.4: Building Model Created in SketchUp Representing the IER Cafeteria Structure with a Volume of 450.5 m^3 , featuring two main windows oriented toward the East and West. Left: Building model facing the exterior window of the building, known as the cafeteria lattice of the IER. This is the window through which the wind enters. Right: Building model facing the interior window of the building, where the wind exits. In both views, two additional windows are visible, each measuring 2.6 meters long by 3.5 meters high, representing the open surfaces of the cafeteria. All windows were modeled as open during the simulation.

- In order to avoid any other variable capable of affecting ideal conditions the wind speed profile layer thickness was also settled to zero.

The zone ventilation was simulated with AirFlowNetwork by the object Detailed Opening and the factors were arranged in favor of keeping the windows entirely open the whole simulation. Also the ventilation control mode was assigned as constant. The result of this configuration is an almost adiabatic thermal zone with two opposite windows while open.

3.2.4 EnergyPlus and adiabatic_mix communication

It is important to set aside a part of this thesis work to explain certain adaptations of the adiabatic_mix function that had to be made to obtain the expected results. These adaptations included the calculation of the convective heat transfer from the zone surfaces and the calculation of the mass flow rate as described in equation 3.14.

The convective heat transfer from the zone surfaces couldn't be eliminated because the convective heat coefficient in EnergyPlus cannot be set to 0. Therefore, it was necessary to add the calculation of this value in the Python function. Its calculation is based on the sum of all heat flows from each surface, which in turn are obtained from the results of the EnergyPlus simulation. The calculation of the mass flow rate is similar; the mass flow rate of infiltration air couldn't be calculated as in EnergyPlus due the complexity of the AFN algorithm, which considers infiltration due to air velocity and thermal buoyancy. However, computing it is not the purpose of this thesis work, so to address this, it was necessary to obtain the value from the EnergyPlus simulation results and then add it to the energy and mass balance in the algorithm coded in Python. Therefore, adiabatic_mix requires the file of the EnergyPlus simulation results to obtain these data and incorporate them into the calculation of the resulting T_{db} and RH from the combination of two air volumes. The validation of adiabatic_mix is based on comparing the results with those of the EnergyPlus simulation, which will be presented in the following chapter.

3.3 Evaporative and adiabatic process

This section presents the methodology for developing the final algorithm that simulates air conditions using a sprayer cooling system. This algorithm combines the two previous ones: Final_Temp, that computes DEC and adiabatic_mix which computes air mixing in an adiabatic space. It aims to replicate the conditions of an open space with sprayers, including external and internal air movement simultaneously, parallel to evaporative cooling from sprayed water. The goal of this algorithm is to compare it with the simulation of the Energy in Buildings group at IEC GEE-IER and analyze if this last one accurately reflects reality.

To achieve this, a function was coded in Python that combines the two functions described earlier, as described in the pseudocode in Algorithm 1.

Algorithm 1 Evaporative cooling and adiabatic mix algorithm

```

Require: dataEP, begin, end, waterEvap
    set_init(dataEp)
    set_end(dataEp)
    set_EvaporationRange
    for i in (dataEP) do
        if EvaporationRange then
             $H_2O = \text{waterEvap}$ 
        else if No EvaporationRange then
             $H_2O = 0$ 
        end if
    end for
    T, w, RH = adiabatic_mix
    T_final, RH_final = FinalTemp(T, RH, H2O)
    return (T_final, RH_final)

```

This function first locates the evaporative range in the EnergyPlus simulation results data using the provided start and end dates. It includes the condition that if the data falls within the evaporation range, there is water available for evaporation; outside this range, the quantity of water to evaporate is 0. After this condition, adiabatic air mixing is performed using the function adiabatic_mix, and then, with the resulting air conditions, the air conditions resulting from the evaporative cooling process are computed with Final_Temp. The results are the air conditions of an air mixed and cooled by the water sprayers.

The logic process that follows this function is the follow one.

1. The air enters to the zone and the adiabatic mixing between the outside and inside air is made.
2. In the evaporation range, 0.7945 grams of water are released within a minute by the sprayers.
3. The dry bulb temperature and the relative humidity results of the evaporative cooling process are calculated.

Once having the algorithm joined and ready, the next step it to compare it with another methodology that simulates an evaporative cooling process by sprayers, such as the one developed by the GEE-IER.

GEE-IER has developed an algorithm to simulate DEC in EnergyPlus. However this algorithm has not been validated. At this point we have two algorithms, the one developed in this thesis that will be validated in the following section and the one developed by the GEE-IER. This last algorithm will be compared with the one validated in this thesis. For this, the IER's algorithm should be applied in a simulation with the specifications from Sec. 3.2.3. The comparison for two experiments will be presented in the following chapter.

Chapter 4

Results

This chapter presents the validation results of the functions developed to simulate the air conditions from the process of a evaporative coolig process by water spayers system and air mixing simultaneously. The validation of the functions developed to calculate air conditions following a direct evaporative cooling process (the spray cooling system) will determine the accuracy of the final dry bulb temperature and final relative humidity of the air. Subsequently, the validation of the adiabatic air mixing function will confirm the accuracy of the energy and mass balance calculations after the mixing between two volumes of air. Following this, the next step is to compare the combined function (which performs both processes) with the simulation process of the GEE-IER. The objective of this comparison is to validate this last one.

4.1 Evaporative cooling process

In order to validate that the direct evaporative cooling by water sprays system calculus were well made, four experiments were performed with the functions Add_water and Final_Temp described in section 3.1. These experiments consist of creating an adiabatic closed volume of air of $1m^3$, with established initial psychrometric conditions (dry bulb temperature, relative humidity, and atmospheric pressure), no ventilation and a specific amount of evaporated water added (quantities detailed on table 3.1) to the air. Subsequently, the final dry bulb temperature and relative humidity were computed using the Add_water and Final_Temp functions (see figures 3.2 and 3.3).

Each experiment had a different initial dry bulb temperature (T_{dbi}), relative humidity (RH_i) and a different amount of evaporated water (ΔH_2O). The results will be compared with an online psychrometric chart (SimCal, 2024). This interactive psychrometric chart, PsychroSim, requires the initial air conditions and the desired process to be simulated in order to perform the calculations. The initial conditions are: Altitude, air flow, dry bulb temperature and relative humidity. The available processes for selection are heating, cooling, air mixing, heat recovery, humidification, and custom point. Since the pressure in the Python functions is set as the atmospheric pressure, the altitude in PsychroSim is set to 0. Additionally, the air flow was set to the minimum allowed, which is $100 m^3/h$. It was observed that this parameter does not affect the results for the selected process, which was humidification for the purpose of the experiment.

Exp.	Function		PsychroSim		
	#	T_{dbf} [°C]	RH_f [%]	T_{dbf} [°C]	RH_f [%]
1		19.8	30.8	19.8	30.8
2		29.8	50.8	29.8	50.8
3		28.8	55.5	28.8	55.5
4		21.9	100	22.2	98.3

Table 4.1: Results of evaporative cooling process experiment

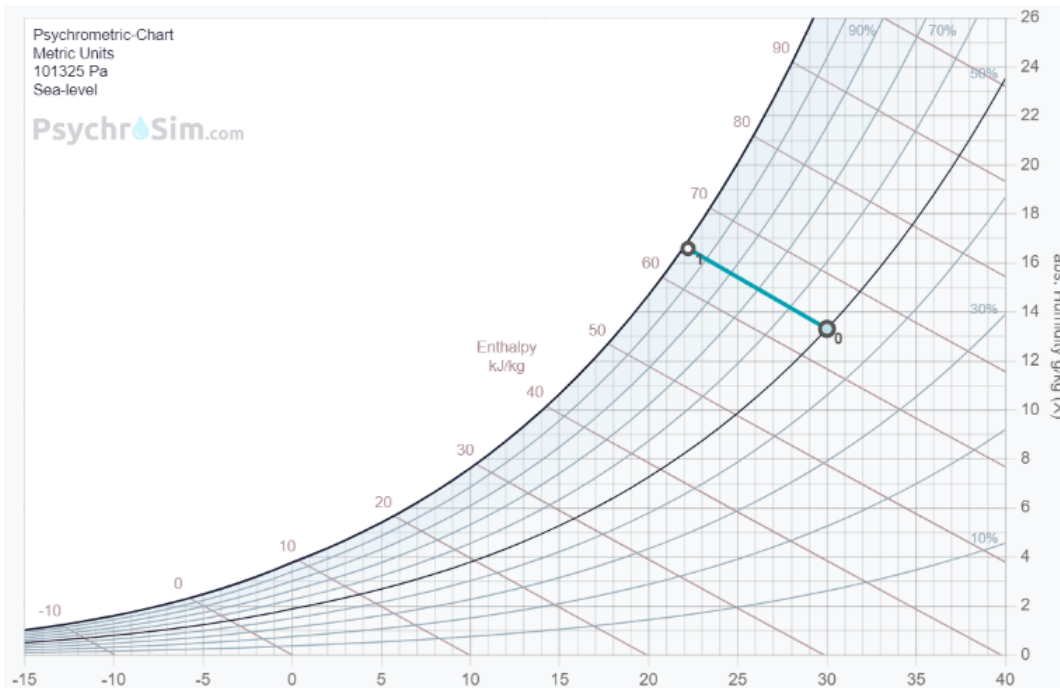


Figure 4.1: Fourth experiment of Evaporative cooling process graphed on the interactive online psychrometric chart PsychroSim.

The table 3.1 shows the initial conditions of dry bulb temperature and relative humidity for the four described experiments, along with the amount of water added by the DEC system. Figure 4.1 presents the results of the fourth experiment graphed on PsychroSim, with the initial state marked as 0 and the result marked as 1. The orientation of the blue line represents an adiabatic process of humidification, leading to a decrease in the dry bulb temperature and an increase in relative humidity. As the fourth experiment intends to saturate the air, the point marked as 1 is located very close to the saturation line.

Table 4.1 presents the results of direct evaporative cooling process using both methods: the functions developed in Python and the interactive online psychrometric chart. As the results provided by PsychroSim are rounded to one decimal, the Python results were also rounded accordingly. It is noticeable that the results of both methods show no differences except for the last one, which is the experiment with the highest amount of evaporated water due to the intend to reach saturation conditions. Despite this representing the most significant temperature change, the error in dry bulb temperature is only 0.3°C and in relative humidity is 1.7%, which is a remarkably low error for such a substantial change. Therefore, it could be concluded that both developed functions, Add_water and Final_Temp, are able to accurately compute direct evaporative cooling. Their validity is confirmed.

4.2 Adiabatic process

This section presents the validation process and results of the adiabatic_mix function described on section 3.2. It was decided to use EnergyPlus as the validation method because it is widely used in research groups and includes the AirFlowNetwork model. AirFlowNetwork can simulate multizone airflows influenced by natural ventilation and/or forced air produced by a HVAC system (Energy, 2022a). Therefore, to compare the results of both methods, it was necessary to simulate an adiabatic thermal zone with air mixing only in EnergyPlus. EnergyPlus simulations, weather files elaboration, and the conducted numerical are presented.

4.2.1 Validation

To validate that adiabatic mixture of two volumes of air were correctly calculated by the Python function developed, adiabatic_mix, and that could return the same results as in EnergyPlus simulation, there were made seven numerical experiments. These experiments consist in setting the initial conditions of dry bulb temperature and relative humidity after a sudden change of one of this variables, computes the inside dry bulb temperature and relative humidity of the adiabatic thermal zone. If both methods give the same results, the energy and mass balance is correctly calculated by the function adiabatic_mix. Every with the same adiabatic space but with different climate conditions:

- Dry bulb temperature, T_{db} [$^{\circ}\text{C}$].
- Relative humidity, RH [%].
- Wind speed, ws [m/s].
- Wind direction, wd [$^{\circ}$].
- Atmospheric pressure, P [Pa]

The climate conditions that can be modified are: dry bulb temperature, relative humidity and wind speed. The atmospheric pressure and wind direction remains constant for each numerical experiment. The wind direction was established at 270° and the atmospheric pressure at 87, 214 Pa. Every experiment starts with the same initial conditions, and then there is a sudden change in a different variable.

These seven experiments are described in the table 4.2. The cells with an arrow detail the variable that had a sudden change and the value shifted. There were experiments that had more than one variable changed at the same time.

In order to establish constant climate conditions for the numerical experiments, EPW files were generated using the EPW file generator tool of EnergyPlus, EnergyPlus Weather converter, with .csv files exported by a written Python notebook. The objective of these files was to establish climate conditions with no heat transfer.

This means that all heat sources such as solar radiation or soil heat conduction were set to zero by default. The variables adjusted were: dry bulb temperature, relative humidity, atmospheric pressure, wind direction, and wind speed. These EPW files last one full year with one-minute time steps. They were initialized with initial climate conditions and, once stable, they have sudden changes in specified variables (depending on the experiment conducted). Once we had these EPW files, we were able to make the validation. For these experiments there were developed seven EPW files, one for each experiment.

Experiment	T_{db} [°C]	RH [%]	ws [m/s]	wd [°]	P [Pa]
1	23 → 24	23	0	270	87,214
2	23 → 40	23	0	270	87,214
3	23	23 → 24	0	270	87,214
4	23	23 → 40	0	270	87,214
5	23 → 24	23	0 → 0.5	270	87,214
6	23	23 → 24	0 → 0.5	270	87,214
7	23 → 24	23 → 24	0 → 0.5	270	87,214

Table 4.2: Adiabatic process experiments

In every EPW file, the atmospheric pressure is constant of 87,214.302 Pa, the wind direction is setted on 270°, pointed westward according to the EnergyPlus manual (Energy, 2022b), and wind speed is 0 except on the experiments where other value of wind speed is mentioned. For each EPW file, the environmental variables that has a sudden change in the experiments are:

- Experiment 1: Dry bulb temperature; changes from 23°C to 24°C in one minute.
- Experiment 2: Dry bulb temperature; changes from 23°C to 40°C in one minute.
- Experiment 3: Relative humidity; changes from 23% to 24% in one minute.
- Experiment 4: Relative humidity; changes from 23% to 40% in one minute.
- Experiment 5: Dry bulb temperature; changes from 23°C to 24°C in one minute.
- Experiment 6: Relative humidity; changes from 23% to 24% in one minute.
- Experiment 7: Dry bulb temperature; changes from 23°C to 24°C in one minute.

To compare the results of both methods (the adiabatic_mix function and EnergyPlus simulation), the results were graphed from figure 4.2 to figure 4.8. Within these graphs the red points are the results calculated by adiabatic_mix function and the blue lines are from EnergyPlus. It is noticed that both methods have the same behavior in each experiment.

Mean absolute error (MAE), standard deviation (std.), and maximum difference (m.d.) of dry bulb temperature and relative humidity were calculated for the seven experiments. These findings are presented in Table 4.3. The results are promising; for the first two experiments where the variable changed was temperature, the MAEs on dry bulb temperature and relative humidity are 3E-3 and 5E-3, respectively, and do not significantly increase even with larger sudden changes. Although the variable modified in these experiments was the dry bulb temperature, the largest maximum differences were in relative humidity, as it is a variable that depends on temperature. The largest standard deviation among these two experiments was observed in the abrupt temperature change from 23°C to 40°C (experiment 2). These two observations indicate that the errors in relative humidity are greater for large changes in dry bulb temperature. However, the maximum difference in relative humidity for experiment 2 was 7.0E-2, which is a fairly acceptable value given the temperature change that had occurred.

For the next two experiments (3 and 4), where the variable modified is relative humidity, errors are of a lower order than temperature but with similarly behaviour. There is no significant error even with larger changes. And it can be observed that changes in relative humidity have less impact on temperature

Exp.	T_{db} [°C]			RH [%]			
	#	MAE	std.	m.d.	MAE	std.	m.d.
1	3.0E-3	1.6E-3	6.0E-3	5.0E-3	2.0E-3	8.0E-3	
2	3.0E-3	1.7E-3	12.0E-3	5.0E-3	5.0E-3	7.0E-2	
3	3.4E-9	1.5E-9	1.9E-8	4.4E-6	1.1E-5	6.6E-5	
4	2.5E-9	6.4E-10	8.2E-9	1.0E-4	8E-4	8.0E-3	
5	1.0E-4	1.0E-4	1.0E-3	2.0E-4	3.0E-4	2.0E-3	
6	3.7E-16	1.3E-15	7.1E-15	2.6E-07	2.3E-6	2.8E-5	
7	1.0E-4	2.0E-4	1.0E-3	2.0E-4	3.0E-4	3.0E-3	

Table 4.3: Mean Absolute Error (MAE), standard desviation (std.) and maximum difference (m.d.) of adiabatic process experiments results.

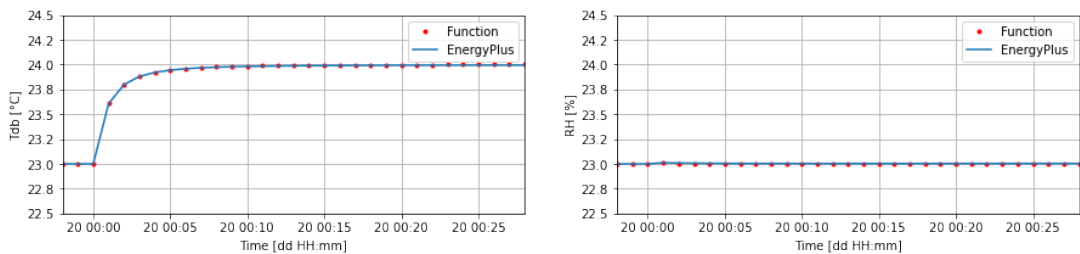


Figure 4.2: Experiment 1 with function adiabatic_mix and EnergyPlus simulation. Left: Inside dry bulb temperature results. Right: Inside relative humidity results.

than vice versa. In the last three experiments, there are no significant changes in dry bulb temperature and relative humidity; instead, the wind speed increases from 0.0 to 0.5 m/s at the same time as the other changes occur. It can be observed that the values of MAE, std., and m.d. are higher when the dry bulb temperature variable changes. However, they are lower when the wind speed increases, compared to previous experiments where the wind speed was 0.0 m/s . These results indicate that the developed function, adiabatic_mix, accurately performs the same computations of air mixing as EnergyPlus. The observed errors could be attributed to the decimal precision that both methods retain from the values.

These results verify that the adiabatic mixture between two air volumes simulated on EnergyPlus was able to be replicated by the function elaborated in Python. Therefore, the second part of the validation process is well established, allowing for the validation of evaporative cooling simulations without the interference of errors in the adiabatic mixture of air.

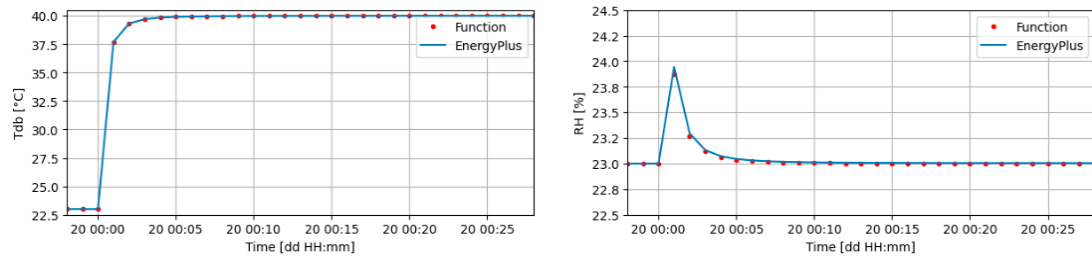


Figure 4.3: Experiment 2 with function adiabatic_mix and EnergyPlus simulation. Left: Inside dry bulb temperature results. Right: Inside relative humidity results.

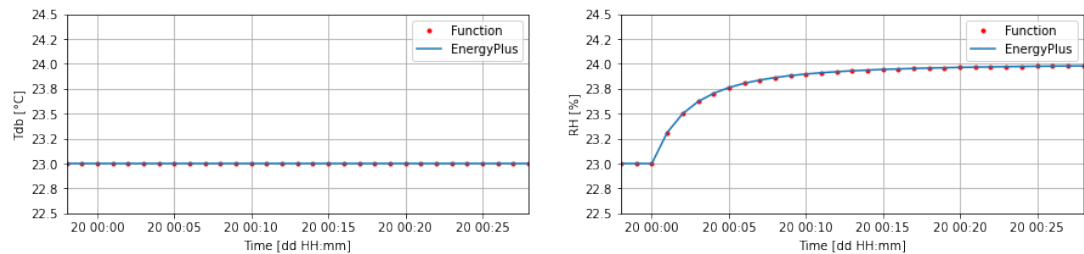


Figure 4.4: Experiment 3 with function adiabatic_mix and EnergyPlus simulation. Left: Inside dry bulb temperature results. Right: Inside relative humidity results.

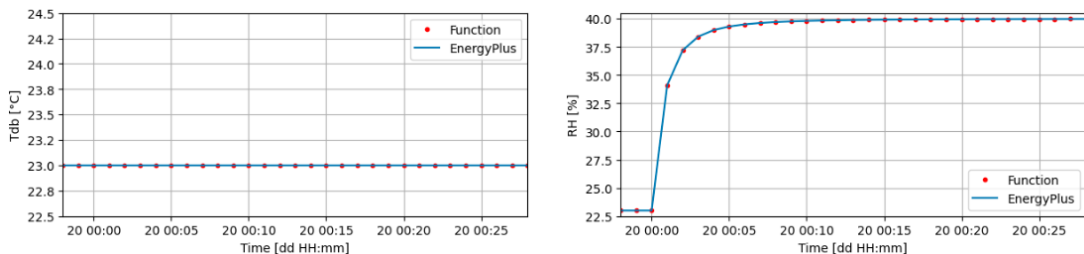


Figure 4.5: Experiment 4 with function adiabatic_mix and EnergyPlus simulation. Left: Inside dry bulb temperature results. Right: Inside relative humidity results.

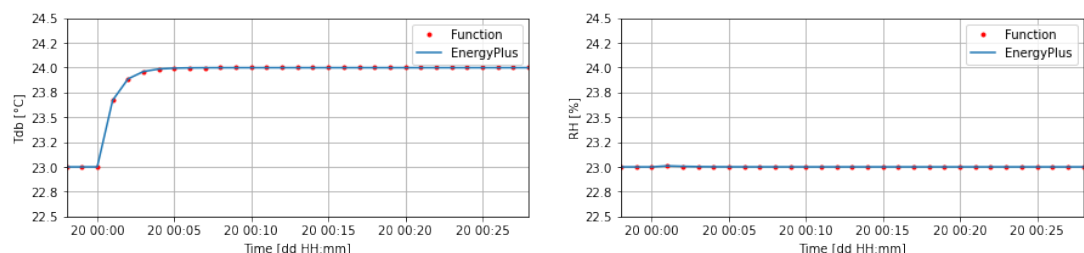


Figure 4.6: Experiment 5 with function adiabatic_mix and EnergyPlus simulation. Left: Inside dry bulb temperature results. Right: Inside relative humidity results.

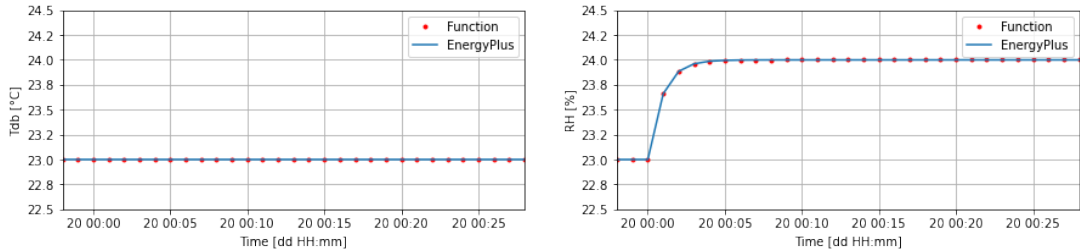


Figure 4.7: Experiment 6 with function adiabatic_mix and EnergyPlus simulation. Left: Inside dry bulb temperature results. Right: Inside relative humidity results.

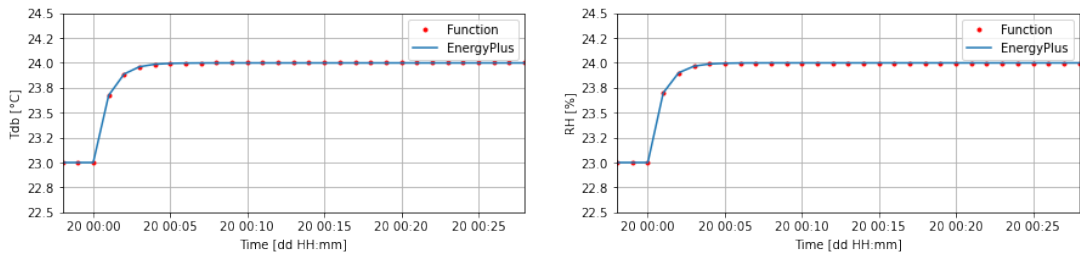


Figure 4.8: Experiment 7 dry bulb temperature and relative humidity results. Left: Inside dry bulb temperature results. Right: Inside relative humidity results.

4.3 Evaporative and adiabatic process

The third part of the validation process consists of the previous two combined; evaporative cooling and adiabatic mix at the same time. For this, a function was developed that combines the evaporative cooling process and the adiabatic air mixture, once both processes were independently validated. This function is described in Section 3.3.

To make a comparison of this function and the simulation process developed by the GEE-IER, two experiments were made. Each experiment consists in making a simulation of an evaporative cooling process within an adiabatic thermal zone with two opposite open windows, therefore with ventilation. For the EnergyPlus simulation, it was used the same methodology developed by the GEE-IER but adapted for this experiment; it was implemented a .py file that computes the air dry bulb temperature and the relative humidity after evaporating water into the air, and a schedule in EnergyPlus linked to an HVAC system that changes the inside dry bulb temperature and relative humidity to the one that the .py file computed.

The first experiment consists of programming the schedule on EnergyPlus and setting the function to evaporate 0.7945 grams of water in one minute at 01:04 hours. The second experiment consists of programming the evaporation of 3.9725 grams of water (0.7945 grams per minute) over five minutes, from 01:04 to 01:09 hours.

For both experiments the environmental conditions in the EPW file were fixed as follows:

- T_{db} : 23°C constant.
- RH : 23% constant.
- ws : 0.0 m/s constant.

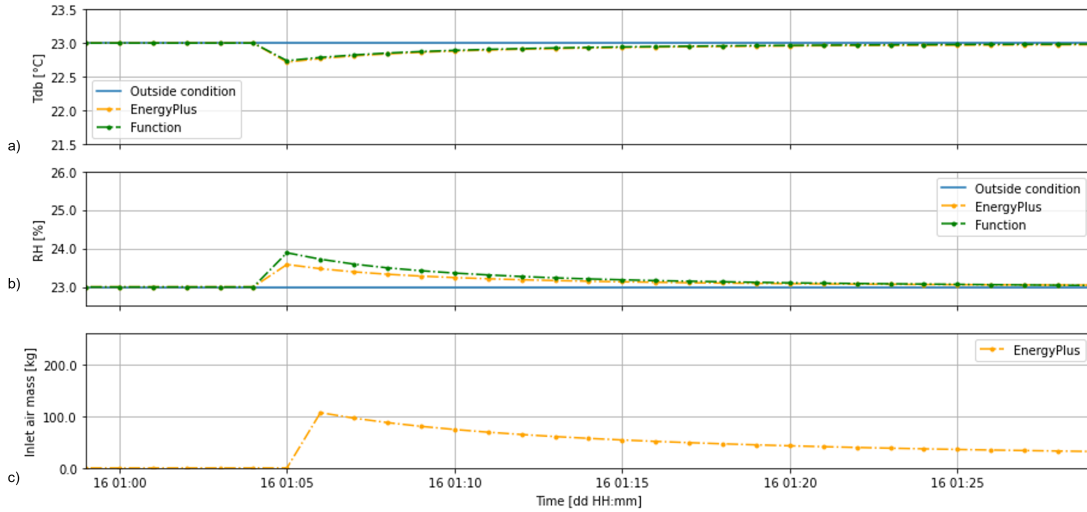


Figure 4.9: Adiabatic mix and evaporative cooling experiments - One minute of evaporation. Blue line are outdoor conditions. Dotted yellow line are indoor conditions computed by .py file in EnergyPlus. Dotted green line are indoor conditions computed by Python function. a) Inside dry bulb temperature behavior. b) Inside relative humidity variable behavior. d) Inlet air mass variable behavior.

- wd : 270° constant.
- P : 87,214.3 Pa constant.

Although it was validated that mass and energy balance is correctly computed, each environmental variable is fixed constant during the entire EPW file in order to observe the evaporative cooling process only.

The graphics in figure 4.9 show the results of inside air dry bulb temperature, inside relative humidity and inlet air mass during a one-minute evaporative cooling process for both methods, the computed by EnergyPlus and the computed by the Python function. It is shown that outdoor variables remain unchanged due to the cooling process occurring indoors. However, air dry bulb temperature and relative humidity do have a noticeable effect produced by both methods; the EnergyPlus computations, with the simulation process developed by GEE-IER, and those carried out by the Python function. Their behaviors appear similar, just with slight differences in the numeric result, more noticeable in relative humidity. Although the variables appear to differ during the evaporative cooling process, they converge to the same values once the cooling process concludes.

In figure 4.10, the graphics for the same experiment over five minutes are presented. Both methods exhibit consistent variable behaviors. Similar to the previous experiment, the precise minute when the cooling process concludes is observed, with variables returning to their initial conditions due to open windows and the airflow network computing the mixing air. However, the differences between the methods in the fifth minute of DEC reached 4.5% in RH and 0.7°C in T_{db} .

The table 4.4 concentrates the mean absolute error, the standard deviation, and the maximum difference between both method's.

At the first time step, the T_{db} reaches a MAE around 1E-4 to 1E-3. It seems that a difference in the

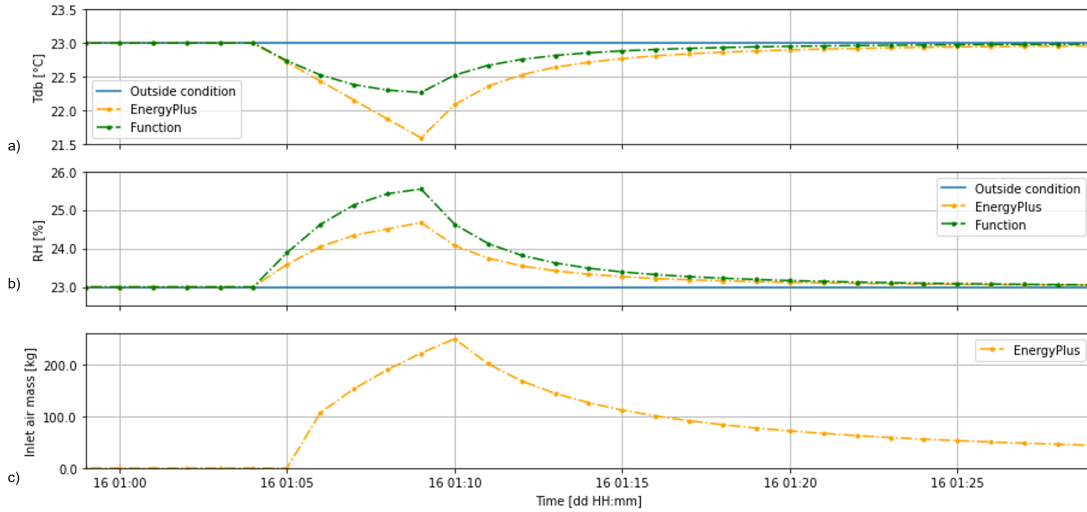


Figure 4.10: Adiabatic mix and evaporative cooling experiments - Five minutes of evaporation. Blue line are outdoor conditions. Dotted yellow line are indoor conditions computed by .py file in EnergyPlus. Dotted green line are indoor conditions computed by Python function. a) Inside dry bulb temperature behavior. b) Inside relative humidity variable behavior. d) Inlet air mass variable behavior.

Experiment		T_{db} [°C]			RH [%]		
#	min.	MAE	std.	m.d.	MAE	std.	m.d.
1	1	1.6E-4	1.1E-3	2.1E-2	1.7E-2	4.5E-3	3.0E-1
2	5	4.6 E-4	9.5E-3	0.7	1.3E-2	1.6E-2	9.2E-1

Table 4.4: Mean Absolute Errors (MAE), standard deviation (std.), and maximum difference (m.d.) for the comparison experiment results of the variables T_{db} and RH .

calculation of RH , which have an MAE of 1.14%, generates an incremental differential in the subsequent values of T_{db} and RH . Therefore, as time progresses, the difference between both methods becomes increasingly larger. Therefore, the difference in the results lies in the calculation of the relative humidity. As emphasized previously, the mass and energy balance is already validated and both methods perform it in the same way. Therefore, this difference could fall on another variable calculated by EnergyPlus with the use of HVAC system.

Chapter 5

Conclusion and Outlook

This thesis work synthesizes the procedure for the development and validation of an algorithm that simulates psychrometric conditions resulting from a direct evaporative cooling process using water sprayers. Likewise, the already validated algorithm was used to compare its results with the DEC simulation process of the GEE-IER. This conclusions chapter summarizes the points of the objectives, their execution process, and whether they were met.

A literature review was conducted on evaporative cooling, the types, existing technologies, and their existing simulation methods, specifically in EnergyPlus. It was concluded that within the types to simulate DEC using sprayers, there is no procedure in this software that fully meets the requirements for its simulation, which is the consideration of multidirectional airflow. Therefore, it would not be possible to obtain reliable results that involve the mixing of air with the outside of the zone and the already cooled air by DEC. The next step was to study and understand the psychrometric calculations for calculating the T_{db} and RH of the air resulting from the DEC. This was the preliminary step and the basis for the development of the methodology and algorithms.

An algorithm was successfully developed that incorporates the evaporation of water and adiabatic mixing in a space. To code an algorithm that meets the requirement for multidirectional airflow mixing, the general process of a DEC in an adiabatic zone was divided into two: the DEC process (with Add_water and Final_Temp function) and the adiabatic air mixture (with adiabatic_mix). Both developed functions were successfully validated. Final_Temp, in the air saturation and cooling experiment of 8.1°C in a single step, obtained a maximum error of 0.3°C in T_{db} and 1.7% in RH with the comparative validation method. Meanwhile, with smaller, less drastic changes and similar to reality experiment, an almost zero error was obtained. The adiabatic_mix function was validated with EnergyPlus by performing a simulation of a nearly adiabatic thermal zone. The calculation of T_{db} and RH after the air mixing was performed using the mass and energy equations utilized by EnergyPlus. However, necessary adjustments were made in adiabatic_mix to compensate for the thermal load that could not be eliminated in the software. The algorithm was also configured to take from EnergyPlus the data of the air mass flow rate of infiltration to the thermal zone due to the complexity of AFN, the EnergyPlus algorithm chosen for calculating air movement. The maximum errors in MAE, std., and m.d. reached values of 10E-3, while the minimum errors were 10E-16, thus adiabatic_mix function was considered validated.

Once validated, the algorithm was used to review the one developed by GEE-IER in EnergyPlus. Two comparison experiments were conducted, one lasting 1 minute and another 5 minutes.

Although both simulation methods exhibited the same behavior, the results diverged more as the evaporation time increased, especially in RH . In the 5-minute experiment, the maximum difference between both simulation processes was 4.5% in RH and 0.7 ° C in T_{db} . Apparently, the dry bulb temperature is correctly computed by the simulation process in EnergyPlus. On the other hand, relative humidity shows an error that causes an incremental difference in the subsequent results. This means the results of both methods become more different according to the evaporation time. This shows that the simulation process of the GEE-IER does not yield correct results the longer the evaporation time. For the following steps, it is necessary to understand the reason for the difference in the EnergyPlus relative humidity calculation and to perform more tests to verify whether the HVAC system causes this difference. Once a validated model is obtained, the GEE-IER's next step will be to compare the results with temperature and humidity measurements taken from a space equipped with a physical sprayer-based evaporative cooling system.

The programming work for the experiments documented in this thesis is saved in an open repository on GitHub. The experiments were conducted in different notebooks, which describe the entire methodology divided into four parts:

- Basic psychrometric aspects of direct evaporative cooling by sprayers.
- DEC process experiments.
- Adiabatic mixing of air experiments.
- DEC and adiabatic mixing of air simultaneously.

This repository is available for consultation for future investigations (Nevárez, 2025).

Acronyms

ACL	Access Control List
CFD	Computational Fluid Dynamics
DEC	Direct Evaporative Cooling
HFMEC	Hollow Fiber Membrane-based Evaporative Cooler
HVAC	Heating, Ventilation, and Air Conditioning
IEC	Indirect Evaporative Cooling
IER	Instituto de Energías Renovables
PDEC	Passive Down-draft Evaporative Cooling
GEE-IER	Energy in Buildings group at IER

Nomenclature

δt	Time interval
δt	Time interval
\dot{m}	Mass flow
\dot{m}	Mass flow
\dot{Q}_i	Internal loads
\dot{Q}_i	Internal loads
$\rho_{\text{air},z}$	Air density in zone
$\rho_{\text{air},z}$	Air density in zone
ρ_{air}	Zone air density
ρ_{air}	Zone air density
A	Surface area
A	Surface area
C_p	Zone air specific heat capacity
C_p	Zone air specific heat capacity
C_T	Sensible heat capacity
C_T	Sensible heat capacity
C_w	Specific heat capacity of air
C_w	Specific heat capacity of air
C_z	Zone air heat capacity
C_z	Zone air heat capacity
C_p	Heat capacity under constant water vapor pressure
C_p	Heat capacity under constant water vapor pressure
h	Enthalpy
h	Enthalpy
h_g	Air enthalpy
h_g	Air enthalpy
h_s	Water vapor enthalpy

h_s	Water vapor enthalpy
$m.d.$	Maximum difference
$m.d.$	Maximum difference
m_a	Mass of dry air
m_a	Mass of dry air
m_g	Maximum amount of water vapor that air can hold at the same temperature as the mass of water
m_g	Maximum amount of water vapor that air can hold at the same temperature as the mass of water
m_s	Mass of water vapor
m_s	Mass of water vapor
m_{splus}	Mass of evaporated water added in a evaporative cooling process
m_{splus}	Mass of evaporated water added in a evaporative cooling process
n	Amount of gas substance
n	Amount of gas substance
P	Pressure
P	Pressure
P_a	Dry air pressure
P_a	Dry air pressure
P_g	Saturated water vapor pressure
P_g	Saturated water vapor pressure
P_s	Water vapor pressure
P_s	Water vapor pressure
R	Ideal gas constant
R	Ideal gas constant
R_s	Water vapor gas constant
R_s	Water vapor gas constant
R_{da}	Dry air gas constant
R_{da}	Dry air gas constant
RH	Relative Humidity
RH	Relative Humidity
$std.$	standard desviation
$std.$	standard desviation
T	Temperature
T	Temperature
t	time
t	time
T_s	Zone surface temperature
T_s	Zone surface temperature
T_z	Thermal zone temperature

T_z	Thermal zone temperature
T_∞	Outside air temperature
T_∞	Outside air temperature
T_{sup}	Supply temperature from a air system output
T_{sup}	Supply temperature from a air system output
T_{as}	Adiabatic saturation temperature
T_{as}	Adiabatic saturation temperature
T_{db}	Dry bulb temperature
T_{db}	Dry bulb temperature
T_{wb}	Wet bulb temperature
T_{wb}	Wet bulb temperature
V	Volumen
V	Volumen
V_z	Zone Volume
V_z	Zone Volume
w	Specific humidity
w	Specific humidity
w_d	Wind direction
w_d	Wind direction
w_s	Wind speed
w_s	Wind speed
W_∞	Moisture content of outside air
W_∞	Moisture content of outside air
MAE	Mean Absolute Error
MAE	Mean Absolute Error

Bibliography

- Alaidroos, A. & M. Krarti (2016). “Experimental validation of a numerical model for ventilated wall cavity with spray evaporative cooling systems for hot and dry climates”. In: *Energy and Buildings* 131, pp. 207–222. ISSN: 0378-7788. DOI: <https://doi.org/10.1016/j.enbuild.2016.09.035>. Available from: <https://www.sciencedirect.com/science/article/pii/S0378778816308702> (cit. on p. 5).
- Alkhedhair, A., H. Gurgenci, I. Jahn, Z. Guan & S. He (2013). “Numerical simulation of water spray for pre-cooling of inlet air in natural draft dry cooling towers”. In: *Applied Thermal Engineering* 61.2, pp. 416–424. ISSN: 1359-4311. DOI: <https://doi.org/10.1016/j.applthermaleng.2013.08.012>. Available from: <https://www.sciencedirect.com/science/article/pii/S135943111300584X> (cit. on p. 5).
- American Society of Heating, R. & A.-C. Engineers (2017). *2017 ASHRAE Handbook: Fundamentals*. 2017th ed. American Society of Heating, Refrigerating and Air-Conditioning Engineers, 2017 (cit. on pp. 12, 14).
- Çengel, Y. A. (2012). *TERMODINÁMICA*. 7th ed. McGRAW-HILL/INTERAMERICANA EDITORES, S.A. DE C.V (cit. on pp. 3, 8).
- Chiesa, G., N. Huberman, D. Pearlmuter & M. Grossi (2017). “Summer Discomfort Reduction by Direct Evaporative Cooling in Southern Mediterranean Areas”. In: *Energy Procedia* 111. 8th International Conference on Sustainability in Energy and Buildings, SEB-16, 11-13 September 2016, Turin, Italy, pp. 588–598. ISSN: 1876-6102. DOI: <https://doi.org/10.1016/j.egypro.2017.03.221>. Available from: <https://www.sciencedirect.com/science/article/pii/S1876610217302515> (cit. on p. 6).
- Duan, Z., X. Zhao, J. Liu & Q. Zhang (2019). “Dynamic simulation of a hybrid dew point evaporative cooler and vapour compression refrigerated system for a build-

- ing using EnergyPlus”. In: *Journal of Building Engineering* 21, pp. 287–301. ISSN: 2352-7102. DOI: <https://doi.org/10.1016/j.jobe.2018.10.028>. Available from: <https://www.sciencedirect.com/science/article/pii/S2352710218305230> (cit. on pp. 4, 6).
- Energy, U. D. of (2022a). *Engineering Reference*. 22.1.0. EnergyPlus™ Version 22.1.0 Documentation (cit. on pp. 15, 23).
- (2022b). *Engineering Reference*. 22.1.0. EnergyPlus (cit. on p. 24).
- GitHub (2024). *psychrolib*. Available from: <https://github.com/psychrometrics/psychrolib> [2024] (cit. on p. 12).
- Huang, C., D. Ye, H. Zhao, T. Liang, Z. Lin, H. Yin & Y. Yang (2011). “The research and application of spray cooling technology in Shanghai Expo”. In: *Applied Thermal Engineering* 31.17. SET 2010 Special Issue, pp. 3726–3735. ISSN: 1359-4311. DOI: <https://doi.org/10.1016/j.aplthermaleng.2011.03.039>. Available from: <https://www.sciencedirect.com/science/article/pii/S1359431111001785> (cit. on p. 5).
- IEA (2023). *Space Cooling*. Available from: <https://www.iea.org/energy-system/buildings/space-cooling> [2023] (cit. on p. 3).
- Jaber, S. & S. Ajib (2011). “Evaporative cooling as an efficient system in Mediterranean region”. In: *Applied Thermal Engineering* 31.14, pp. 2590–2596. ISSN: 1359-4311. DOI: <https://doi.org/10.1016/j.aplthermaleng.2011.04.026>. Available from: <https://www.sciencedirect.com/science/article/pii/S1359431111002249> (cit. on p. 4).
- Jafari, S. & V. Kalantar (2022). “Numerical simulation of natural ventilation with passive cooling by diagonal solar chimneys and windcatcher and water spray system in a hot and dry climate”. In: *Energy and Buildings* 256, p. 111714. ISSN: 0378-7788. DOI: <https://doi.org/10.1016/j.enbuild.2021.111714>. Available from: <https://www.sciencedirect.com/science/article/pii/S0378778821009981> (cit. on p. 5).
- Kang, D. & R. K. Strand (2013). “Modeling of simultaneous heat and mass transfer within passive down-draft evaporative cooling (PDEC) towers with spray in FLUENT”. In: *Energy and Buildings* 62, pp. 196–209. ISSN: 0378-7788. DOI: <https://doi.org/10.1016/j.enbuild.2013.02.039>. Available from: <https://www.sciencedirect.com/science/article/pii/S0378778813001278> (cit. on p. 5).
- (2018). “Performance control of a spray passive down-draft evaporative cooling system”. In: *Applied Energy* 222, pp. 915–931. ISSN: 0306-2619. DOI: <https://doi.org/10.1016/j.apenergy.2018.03.039>. Available from:

- <https://www.sciencedirect.com/science/article/pii/S0306261918303660> (cit. on p. 6).
- Kang, D. & R. K. Strand (2019). “Analysis of the system response of a spray passive downdraft evaporative cooling system”. In: *Building and Environment* 157, pp. 101–111. ISSN: 0360-1323. DOI: <https://doi.org/10.1016/j.buildenv.2019.04.037>. Available from: <https://www.sciencedirect.com/science/article/pii/S0360132319302896> (cit. on pp. 4, 6).
- Laboratory, N. R. E. (2025). *EnergyPlus*. Available from: <https://energyplus.net/> [2025] (cit. on p. 1).
- Luigi Gentile Polese (Aug. 28, 2014). *EnergyPlus*. Available from: <https://www.energy.gov/eere/buildings/articles/energyplus> [Feb. 22, 2024] (cit. on p. 6).
- Meng, X., L. Meng, Y. Gao & H. Li (2022). “A comprehensive review on the spray cooling system employed to improve the summer thermal environment: Application efficiency, impact factors, and performance improvement”. In: *Building and Environment* 217, p. 109065. ISSN: 0360-1323. DOI: <https://doi.org/10.1016/j.buildenv.2022.109065>. Available from: <https://www.sciencedirect.com/science/article/pii/S0360132322003043> (cit. on pp. 3, 4).
- Meyer, D. & D. Thevenard (2019). “PsychroLib: a library of psychrometric functions to calculate thermodynamic properties of air”. In: *The Journal of Open Source Software* 4, p. 1137. DOI: <https://doi.org/10.21105/joss.01137>. Available from: <https://joss.theoj.org/papers/10.21105/joss.01137> (cit. on p. 12).
- Mohammad, A. T., S. B. Mat, M. Sulaiman, K. Sopian & A. A. Al-abidi (2013). “Historical review of liquid desiccant evaporation cooling technology”. In: *Energy and Buildings* 67, pp. 22–33. ISSN: 0378-7788. DOI: <https://doi.org/10.1016/j.enbuild.2013.08.018>. Available from: <https://www.sciencedirect.com/science/article/pii/S037877881300515X> (cit. on pp. 3, 5).
- Naderi, E., B. Sajadi, E. Naderi & B. Bakhti (2020). “Simulation-based performance analysis of residential direct evaporative coolers in four climate regions of Iran”. In: *Journal of Building Engineering* 32, p. 101514. ISSN: 2352-7102. DOI: <https://doi.org/10.1016/j.jobe.2020.101514>. Available from: <https://www.sciencedirect.com/science/article/pii/S235271022030824X> (cit. on p. 6).

- Nevárez, J. (2025). *ThesisEvaporativeCoolingFinalResults*. Available from: https://github.com/jessineva/Thesis_EvaporativeCooling_Final_Results.git [2025] (cit. on p. 31).
- Raoult, F., S. Lacour, B. Carissimo, F. Trinquet, A. Delahaye & L. Fournaison (2019). “CFD water spray model development and physical parameter study on the evaporative cooling”. In: *Applied Thermal Engineering* 149, pp. 960–974. ISSN: 1359-4311. DOI: <https://doi.org/10.1016/j.applthermaleng.2018.12.063>. Available from: <https://www.sciencedirect.com/science/article/pii/S1359431118327686> (cit. on p. 5).
- Santamouris, M. & D. Kolokotsa (2013). “Passive cooling dissipation techniques for buildings and other structures: The state of the art”. In: *Energy and Buildings* 57, pp. 74–94. ISSN: 0378-7788. DOI: <https://doi.org/10.1016/j.enbuild.2012.11.002>. Available from: <https://www.sciencedirect.com/science/article/pii/S0378778812005762> (cit. on pp. 3–5).
- SimCal (2024). *PsychroSim.com | Calc Sketch*. Available from: <https://www.psychrosim.com/> [2024] (cit. on pp. 14, 21).
- Al-Sulaiman, F. (2002). “Evaluation of the performance of local fibers in evaporative cooling”. In: *Energy Conversion and Management* 43.16, pp. 2267–2273. ISSN: 0196-8904. DOI: [https://doi.org/10.1016/S0196-8904\(01\)00121-2](https://doi.org/10.1016/S0196-8904(01)00121-2). Available from: <https://www.sciencedirect.com/science/article/pii/S0196890401001212> (cit. on p. 4).
- Tewari, P., S. Mathur & J. Mathur (2019). “Thermal performance prediction of office buildings using direct evaporative cooling systems in the composite climate of India”. In: *Building and Environment* 157, pp. 64–78. ISSN: 0360-1323. DOI: <https://doi.org/10.1016/j.buildenv.2019.04.044>. Available from: <https://www.sciencedirect.com/science/article/pii/S0360132319302963> (cit. on p. 6).
- Yan, W., X. Meng, X. Cui, Y. Liu, Q. Chen & L. Jin (2022). “Evaporative cooling performance prediction and multi-objective optimization for hollow fiber membrane module using response surface methodology”. In: *Applied Energy* 325, p. 119855. ISSN: 0306-2619. DOI: <https://doi.org/10.1016/j.apenergy.2022.119855>. Available from: <https://www.sciencedirect.com/science/article/pii/S0306261922011229> (cit. on p. 6).
- Zhang, Q., S. He, J. Cheng, B. Zhao, X. Wu, M. Yan, M. Gao, Z. Geng & S. Zhang (2022). “Numerical simulation of evaporative cooling process in a medium-gap-medium arrangement”. In: *International Journal of Thermal Sciences* 179, p. 107700. ISSN: 1290-0729. DOI: <https://doi.org/10.1016/j.ijthermalsci.2022.107700>.

2022.107700. Available from: <https://www.sciencedirect.com/science/article/pii/S1290072922002356> (cit. on pp. 4, 5).